The asymmetric Goos–Hänchen effect

2014 J. Opt. 16 015702

(http://iopscience.iop.org/2040-8986/16/1/015702)

IOP Publishing Journal of Optics
J. Opt. **16** (2014) 015702 (7pp) doi:10.1088/2040-8978/16/1/015702

The asymmetric Goos–Hänchen effect

Manoel P Araujo[1], **Silvânia A Carvalho**[2] **and Stefano De Leo**[2]

[1] Gleb Wataghin Physics Institute, State University of Campinas, Brazil
[2] Department of Applied Mathematics, State University of Campinas, Brazil

E-mail: deleo@ime.unicamp.br

Received 24 September 2013, accepted for publication 24 October 2013
Published 18 November 2013

Abstract
We show under which conditions optical Gaussian beams, propagating throughout an homogeneous dielectric right angle prism, present an *asymmetric* Goos–Hänchen (GH) effect. This asymmetric behavior is seen for incidence at critical angles and happens in the propagation direction of the outgoing beam. The asymmetric GH effect can also be seen as an *amplification* of the standard GH shift. Due to the fact that it only depends on the ratio between the wavelength and the minimal waist size of the incoming Gaussian beam, it can also be used to determine one of these parameters. Multiple-peak interference is an additional phenomenon seen in the presence of such asymmetric effects.

Keywords: Goos–Hanchen shift, Gaussian beams

(Some figures may appear in colour only in the online journal)

1. Introduction

The behavior of laser Gaussian beams in the presence of *symmetric* and *asymmetric* wavenumber distributions is the subject matter of this paper. The importance of the difference among such kinds of distributions can be understood if one takes into account the analogy between optics [1, 2] and non-relativistic quantum mechanics [3, 4] and discusses the behavior between *stationary* and *dynamical* maxima.

A non-relativistic free (Gaussian) particle in its rest frame is described by the following wavepacket:

$$\begin{aligned}\Psi(x,y,t) &= \Psi_0 \frac{d}{4\pi}\int_{-\infty}^{+\infty} \mathrm{d}k_x \int_{-\infty}^{+\infty} \mathrm{d}k_y \\ &\quad\times \exp\left[-\frac{(k_x^2+k_y^2)d^2}{4}\right. \\ &\quad\left.+\,\mathrm{i}\left(k_x x + k_y y - \hbar\frac{k_x^2+k_y^2}{2m}t\right)\right] \\ &= \Psi_0 \mathcal{G}\left(\frac{x}{d},\frac{\hbar t}{md^2}\right)\mathcal{G}\left(\frac{y}{d},\frac{\hbar t}{md^2}\right), \qquad (1)\end{aligned}$$

where

$$\mathcal{G}(\alpha,\beta) = \exp\left[-\frac{\alpha^2}{1+2\mathrm{i}\beta}\right]\Big/\sqrt{1+2\mathrm{i}\beta}.$$

This wave convolution is the solution of the two-dimensional Schrödinger equation [3]

$$\left[\partial_{xx}+\partial_{yy}+2\mathrm{i}\frac{m}{\hbar}\partial_t\right]\Psi(x,y,t)=0. \qquad (2)$$

The Gaussian probability density, $|\Psi(x,y,t)|^2$, grows with the beam diameter as a function of time. Its maximum, which decreases for increasing values of time, is *always* located at $x=y=0$. It represents a *stationary* maximum. It is obvious that the previous analysis is a consequence of the choice of a *symmetric* momentum distribution centered at $k_x=k_y=0$.

To illustrate the idea behind our study, let us consider a Gaussian momentum distribution with only positive momentum values for k_y, i.e.

$$\begin{aligned}\Phi(x,y,t) &= \Phi_0 \mathcal{G}\left(\frac{x}{d},\frac{\hbar t}{md^2}\right)\frac{d}{\sqrt{\pi}}\int_0^{+\infty}\mathrm{d}k_y \\ &\quad\times \exp\left[-\frac{k_y^2 d^2}{4}+\mathrm{i}k_y y-\mathrm{i}\hbar\frac{k_y^2}{2m}t\right] \\ &= \Phi_0 \mathcal{G}\left(\frac{x}{d},\frac{\hbar t}{md^2}\right)\mathcal{G}\left(\frac{y}{d},\frac{\hbar t}{md^2}\right) \\ &\quad\times\left[1+\mathrm{erf}\left(\mathrm{i}\frac{y}{d}\Big/\sqrt{1+\mathrm{i}\frac{2\hbar t}{md^2}}\right)\right]. \qquad (3)\end{aligned}$$

The maximum of this distribution can be estimated by using a basic principle of asymptotic analysis [5]. For oscillatory integrals, the rapid oscillation over the range of integration means that the integrand averages to zero. To avoid this cancelation rule, the phase has to be calculated when it is stationary, i.e.

$$0 = \left\{ \frac{\partial}{\partial k_y} \left[k_y y - \hbar \frac{k_y^2}{2m} t \right] \right\}_{k_y = \langle k_y \rangle} \Rightarrow y = \frac{\hbar \langle k_y \rangle}{m} t.$$

The *breaking* of symmetry in the Gaussian momentum distribution implies now an expected value of k_y different from zero:

$$\langle k_y \rangle = \int_0^{+\infty} \mathrm{d}k_y \, k_y \exp\left[-\frac{k_y^2 d^2}{4} \right] \Big/ \int_0^{+\infty} \mathrm{d}k_y \times \exp\left[-\frac{k_y^2 d^2}{4} \right] = \frac{2}{d\sqrt{\pi}}, \tag{4}$$

and, consequently, a *dynamical* maximum at

$$y_{\max} = \frac{2\hbar}{md\sqrt{\pi}} t. \tag{5}$$

For non-relativistic quantum particles, the difference between stationary and dynamical maxima can be roughly represented as the difference between symmetric and asymmetric wavenumber distributions. The aim of this paper is to investigate under which conditions we can reproduce dynamical maxima for laser Gaussian beams propagating throughout a homogeneous dielectric right angle prism.

The Maxwell equations

$$\left[\nabla^2 - \frac{\partial_{\mathrm{tt}}}{c^2} \right] E(\boldsymbol{r}, t) = 0, \tag{6}$$

for time harmonic electric fields ($\exp[-\mathrm{i}\omega t]$) and for plane waves, modulated by a complex amplitude $A(\boldsymbol{r})$, which travel along the z-direction ($\exp[\mathrm{i}kz]$ with $k = \omega/c = 2\pi/\lambda$),

$$E(\boldsymbol{r}, t) = E_0 \mathrm{e}^{\mathrm{i}(kz - \omega t)} A(\boldsymbol{r}),$$

reduce to [6]

$$\begin{aligned} 0 &= E_0 \mathrm{e}^{\mathrm{i}(kz-\omega t)} \left[\partial_{xx} + \partial_{yy}\partial_{zz} + 2\mathrm{i}k\partial_z - k^2 + \frac{\omega^2}{c^2} \right] A(\boldsymbol{r}) \\ &= E_0 \mathrm{e}^{\mathrm{i}(kz-\omega t)} \left[\partial_{xx} + \partial_{yy} + \partial_{zz} + 2\mathrm{i}k\partial_z \right] A(\boldsymbol{r}). \end{aligned} \tag{7}$$

In the paraxial approximation [1], $A(\boldsymbol{r})$ is a slowly varying function of z and the previous equation becomes

$$\left[\partial_{xx} + \partial_{yy} + 2\mathrm{i}k\partial_z \right] A(x, y, z) = 0. \tag{8}$$

The analogy between the paraxial approximation of the Maxwell equations, equation (8), and the non-relativistic Schrödinger equation, equation (2), is then clear if we consider the following correspondence rules [7, 8]:

$$z \longleftrightarrow t \qquad \text{and} \qquad k \longleftrightarrow m/\hbar.$$

It is interesting to ask in which circumstances, by using optical paraxial beams, it is possible to have an asymmetrical wavenumber distribution and, consequently, produce a dynamical shift. The study presented in this paper aims to give a satisfactory answer to this intriguing question.

Gaussian beams are the simplest kinds of paraxial beams provided by a laser source. The electric field amplitude of the incident paraxial Gaussian beam is given by [9, 10]

$$\begin{aligned} E(\boldsymbol{r}, t) &= E_0 \mathrm{e}^{\mathrm{i}(kz-\omega t)} \frac{\mathrm{w}_0^2}{4\pi} \int_{-\infty}^{+\infty} \mathrm{d}k_x \int_{-\infty}^{+\infty} \mathrm{d}k_y \\ &\quad \times \exp\left[-\frac{(k_x^2 + k_y^2)\mathrm{w}_0^2}{4} + \mathrm{i}\left(k_x x + k_y y - \frac{k_x^2 + k_y^2}{2k} z \right) \right] \\ &= E_0 \mathrm{e}^{\mathrm{i}(kz-\omega t)} A(\boldsymbol{r}), \end{aligned} \tag{9}$$

where w_0 is the minimal waist size of the beam. After performing the k_x and k_y integrations, we obtain

$$A(\boldsymbol{r}) = \mathcal{G}\left(\frac{x}{\mathrm{w}_0}, \frac{z}{k\mathrm{w}_0^2} \right) \mathcal{G}\left(\frac{y}{\mathrm{w}_0}, \frac{z}{k\mathrm{w}_0^2} \right). \tag{10}$$

The density probability distribution of the Gaussian electric field,

$$|E(\boldsymbol{r}, t)|^2 = |E_0|^2 \left[\frac{\mathrm{w}_0}{\mathrm{w}(z)} \right]^2 \exp\left[-2\frac{x^2 + y^2}{w^2(z)} \right], \tag{11}$$

grows with the beam diameter as a function of the z-distance from the beam waist w_0:

$$\mathrm{w}(z) = \mathrm{w}_0 \sqrt{1 + \left(\frac{2z}{k\mathrm{w}_0} \right)^2}.$$

The maximum, which decreases for increasing values of z, is always located at $x = y = 0$. This maximum plays the role of the *stationary* maximum for the quantum non-relativistic particle in its rest frame.

In this paper, we investigate the behavior of optical Gaussian beams which propagate through a right angle prism; see figure 1. For incidence angle $\theta > \theta_{\mathrm{c}}$, the beam is totally reflected at the second interface, and its wavenumber distribution is *symmetric* and centered at $k_x = k_y = 0$. Consequently, the Goos–Hänchen shift [11] is *stationary* in the direction of the beam propagation. The optical phenomenon in which linearly polarized light undergoes a small phase shift, $\delta \approx \lambda$, when totally internally reflected is widely investigated in the literature [12–19]. For incidence at and near critical angles [20–22], we find a frequency crossover in the GH shift which leads to an amplification effect, $\delta_{\mathrm{c}} \approx \sqrt{k\mathrm{w}_0}\lambda$. In this paper, we shall present a *new* effect for incidence at critical angles. Depending on the magnitude of $k\mathrm{w}_0$, *only* the positive values of k_y, in the wavenumber distribution, contribute to reflection and this *asymmetry* produces a *dynamical* Goos–Hänchen shift. It is thus the breaking of the symmetry in the wavenumber distribution which opens the door to a dynamical maximum.

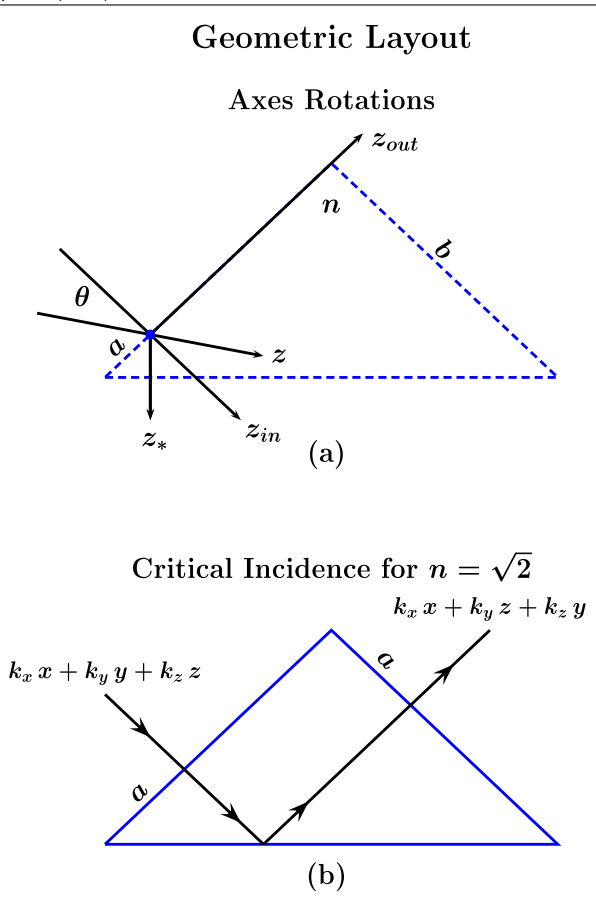

Figure 1. Geometric layout of the dielectric structure analyzed in this paper.

A detailed analysis of this new phenomenon will be discussed in section 3. Before of our numerical study, in section 2, we introduce our notation and the geometry of the dielectric system used in this paper. In this section, we also give, for s- and p-polarized waves, the reflection and transmission coefficients at each interface. Our final considerations and proposals are given in section 4.

2. The dielectric system geometry and outgoing beam

The incident Gaussian beam (9) propagates along the z-axis and forms an angle θ with $z_{\rm in}$, normal to the first air/dielectric interface (see figure 1(a)):

$$\begin{pmatrix} y_{\rm in} \\ z_{\rm in} \end{pmatrix} = \begin{pmatrix} \cos\theta & \sin\theta \\ -\sin\theta & \cos\theta \end{pmatrix} \begin{pmatrix} y \\ z \end{pmatrix} = R(\theta) \begin{pmatrix} y \\ z \end{pmatrix}. \qquad (12)$$

Observing that the spatial phase of the incoming beam is

$$\boldsymbol{k}_{\rm in} \cdot \boldsymbol{r}_{\rm in} = \boldsymbol{k} \cdot \boldsymbol{r}, \qquad (13)$$

with $k_z = k - (k_x^2 + k_y^2)/2k$, we obtain, for the beam propagating within the dielectric after the first air/dielectric interface, the following phase:

$$\boldsymbol{q}_{\rm in} \cdot \mathbf{r}_{\rm in} = k_x x + k_{y_{\rm in}} y_{\rm in} + \sqrt{n^2 k^2 - k_x^2 - k_{y_{\rm in}}^2}\, z_{\rm in}. \qquad (14)$$

In order to follow the beam motion within the dielectric, we have to introduce two new rotations of the axes (see figure 1(a)):

$$\begin{pmatrix} y_{\rm out} \\ z_{\rm out} \end{pmatrix} = R\left(-\frac{3\pi}{4}\right) \begin{pmatrix} y_* \\ z_* \end{pmatrix} = R\left(-\frac{\pi}{2}\right) \begin{pmatrix} y_{\rm in} \\ z_{\rm in} \end{pmatrix}, \qquad (15)$$

with z_* and $z_{\rm out}$ respectively normal to the second and third dielectric/air interfaces. The spatial phase of the beam moving within the dielectric in the direction of the last dielectric/air discontinuity can be given in terms of the outgoing axes:

$$\boldsymbol{q}_{\rm out} \cdot \mathbf{r}_{\rm out} = k_x x + q_{y_{\rm out}} y_{\rm out} + q_{z_{\rm out}} z_{\rm out}, \qquad (16)$$

where

$$\begin{pmatrix} q_{y_{\rm out}} \\ q_{z_{\rm out}} \end{pmatrix} = R\left(-\frac{3\pi}{4}\right) \begin{pmatrix} q_{y_*} \\ -q_{z_*} \end{pmatrix} = \begin{pmatrix} -k_{y_{\rm in}} \\ q_{z_{\rm in}} \end{pmatrix}.$$

Observe that the spatial phase of the reflected beam at the second dielectric/air interface is obtained replacing q_{z_*} by $-q_{z_*}$. Finally,

$$\begin{aligned} \mathbf{k}_{\rm out} \cdot \mathbf{r}_{\rm out} &= k_x x + q_{y_{\rm out}} y_{\rm out} + \sqrt{k^2 - k_x^2 - q_{y_{\rm out}}^2}\, z_{\rm out} \\ &= k_x x + k_{y_{\rm in}} z_{\rm in} + k_{z_{\rm in}} y_{\rm in} \\ &= k_x x + [k_z \cos(2\theta) - k_y \sin(2\theta)] y \\ &\quad + [k_z \sin(2\theta) + k_y \cos(2\theta)] z, \end{aligned} \qquad (17)$$

As expected from the Snell law [1, 2],

$$[\nabla(\mathbf{k}_{\rm out} \cdot \mathbf{r}_{\rm out})]_{(k_x=0,k_y=0)} = [0, k\cos(2\theta), k\sin(2\theta)]. \qquad (18)$$

The amplitude of the outgoing beam is given by [9, 10]

$$\begin{aligned} A_{\rm out}^{[s,p]}(\boldsymbol{r}, \theta) = \frac{w_0^2}{4\pi} \int_{-\infty}^{+\infty} {\rm d}k_x \int_{-\infty}^{+\infty} {\rm d}k_y\, T_\theta^{[s,p]}(k_x, k_y) \\ \times \exp\left[-\frac{(k_x^2 + k_y^2) w_0^2}{4} \right. \\ \left. + {\rm i}\varphi_{\rm out}(k_x, k_y; \boldsymbol{r}, \theta) \right], \end{aligned} \qquad (19)$$

where

$$\begin{aligned} \varphi_{\rm out}(k_x, k_y; \boldsymbol{r}, \theta) = k_x x + k_y[\cos(2\theta) z - \sin(2\theta) y] \\ - \frac{k_x^2 + k_y^2}{2k}[\cos(2\theta) y + \sin(2\theta) z] \end{aligned}$$

and $T_\theta^{[s,p]}(k_x, k_y)$ are obtained by calculating the reflection and transmission coefficients at each interface. For s-polarized waves, this means that

$$\begin{aligned} &\frac{2k_{z_{\rm in}}}{k_{z_{\rm in}} + q_{z_{\rm in}}} \times \frac{q_{z_*} - k_{z_*}}{q_{z_*} + k_{z_*}} \exp[2{\rm i} q_{z_*} a_*] \\ &\times \frac{2q_{z_{\rm out}}}{q_{z_{\rm out}} + k_{z_{\rm out}}} \exp[{\rm i}(q_{z_{\rm out}} - k_{z_{\rm out}}) a_{\rm out}]. \end{aligned}$$

By using the geometry of the dielectric system (see figure 1(a) and equations (16) and (17)), we obtain

$$a_* = a/\sqrt{2}, \qquad a_{\rm out} = b - a,$$
$$q_{z_{\rm out}} = q_{z_{\rm in}} \qquad \text{and} \qquad k_{z_{\rm out}} = k_{z_{\rm in}}.$$

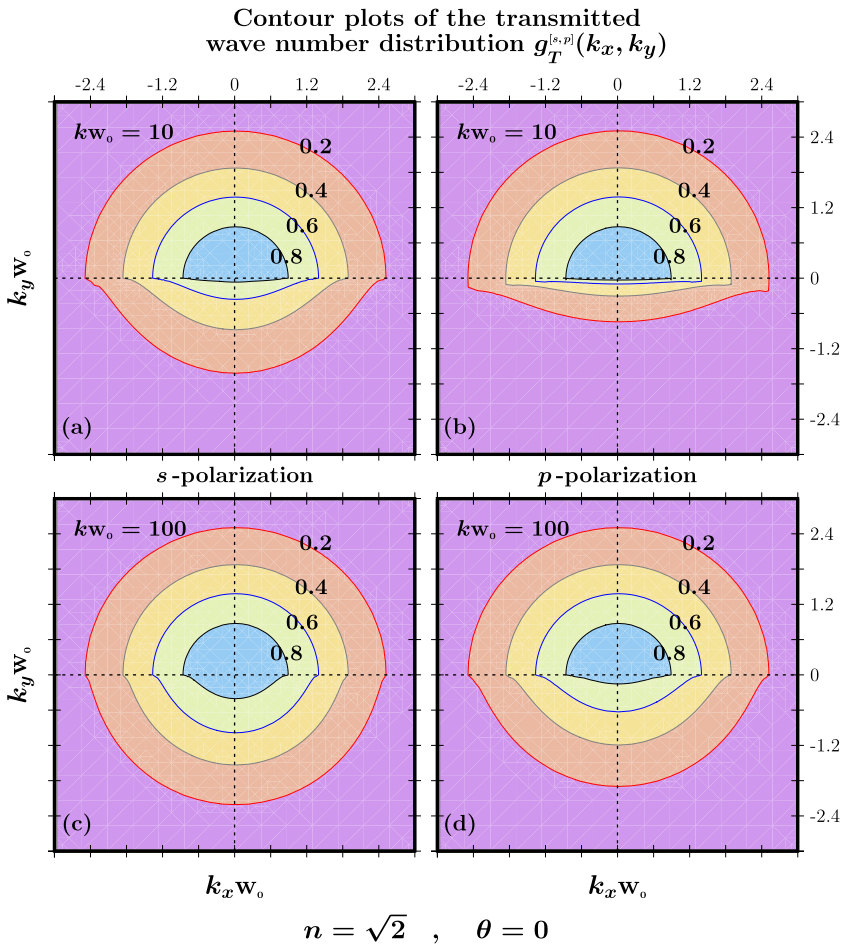

Figure 2. Contour plots of the transmitted wavenumber distribution, $g_T(k_x, k_y)$, at the critical angle for increasing values of kw_0. The numerical data show that the symmetry, which is broken for $kw_0 = 10$, is recovered by increasing the value of kw_0 (total internal reflection).

Consequently, the transmission coefficient becomes

$$T_\theta^{[s]}(k_x, k_y) = \frac{4k_{z_{in}} q_{z_{in}}}{(k_{z_{in}} + q_{z_{in}})^2} \frac{q_{z_*} - k_{z_*}}{q_{z_*} + k_{z_*}} \exp\{i[q_{z_*} a\sqrt{2} + (q_{z_{in}} - k_{z_{in}})(b - a)]\}. \quad (20)$$

For p-polarized waves, we find

$$T_\theta^{[p]}(k_x, k_y) = \frac{4n^2 k_{z_{in}} q_{z_{in}}}{(n^2 k_{z_{in}} + q_{z_{in}})^2} \frac{q_{z_*} - n^2 k_{z_*}}{q_{z_*} + n^2 k_{z_*}} \exp\{i[q_{z_*} \times a\sqrt{2} + (q_{z_{in}} - k_{z_{in}})(b - a)]\}. \quad (21)$$

Due to the fact that the motion is on the y–z plane, only second-order k_x-contributions appear in the transmission coefficient, $T_\theta^{[s,p]}(k_x, k_y)$. Thus, without loss of generality, to calculate the complex amplitude $A_{out}^{[s,p]}(\boldsymbol{r}, \theta)$ we can adopt the following approximation: $T_\theta^{[s,p]}(k_x, k_y) \approx T_\theta^{[s,p]}(0, k_y)$. Consequently,

$$A_{out}^{[s,p]}(\boldsymbol{r}, \theta) \approx \frac{w_0^2}{4\pi} \int_{-\infty}^{+\infty} dk_x \int_{-\infty}^{+\infty} dk_y \, T_\theta^{[s,p]}(0, k_y) \times \exp\left[-\frac{(k_x^2 + k_y^2) w_0^2}{4} + i\varphi_{out}(k_x, k_y; \boldsymbol{r}, \theta)\right]$$

$$= \mathcal{G}\left[\frac{x}{w_0}, \frac{\cos(2\theta) y + \sin(2\theta) z}{z_R}\right] \times \mathcal{F}_\theta^{[s,p]}(y, z), \quad (22)$$

where

$$\mathcal{F}_\theta^{[s,p]}(y, z) = \frac{w_0}{2\sqrt{\pi}} \int_{-\infty}^{+\infty} dk_y \, T_\theta^{[s,p]}(0, k_y) \times \exp\left[-\frac{k_y^2 w_0^2}{4} + i\varphi_{out}(0, k_y; \boldsymbol{r}, \theta)\right].$$

The detailed analysis of $\mathcal{F}_\theta^{[s,p]}(y, z)$ will be the subject matter of section 3.

3. The asymmetric GH effect and multiple-peak interference

Let us consider the momentum distribution

$$g_T^{[s,p]}(k_x, k_y) = T_\theta^{[s,p]}(0, k_y) \exp\left[-\frac{(k_x^2 + k_y^2) w_0^2}{4}\right] \quad (23)$$

responsible for the shape of the transmitted beam. The contour plots of $g_T(k_x, k_y)^{[s,p]}$ clearly show that for decreasing value of kw_0, see figure 2, and for incidence angles approaching

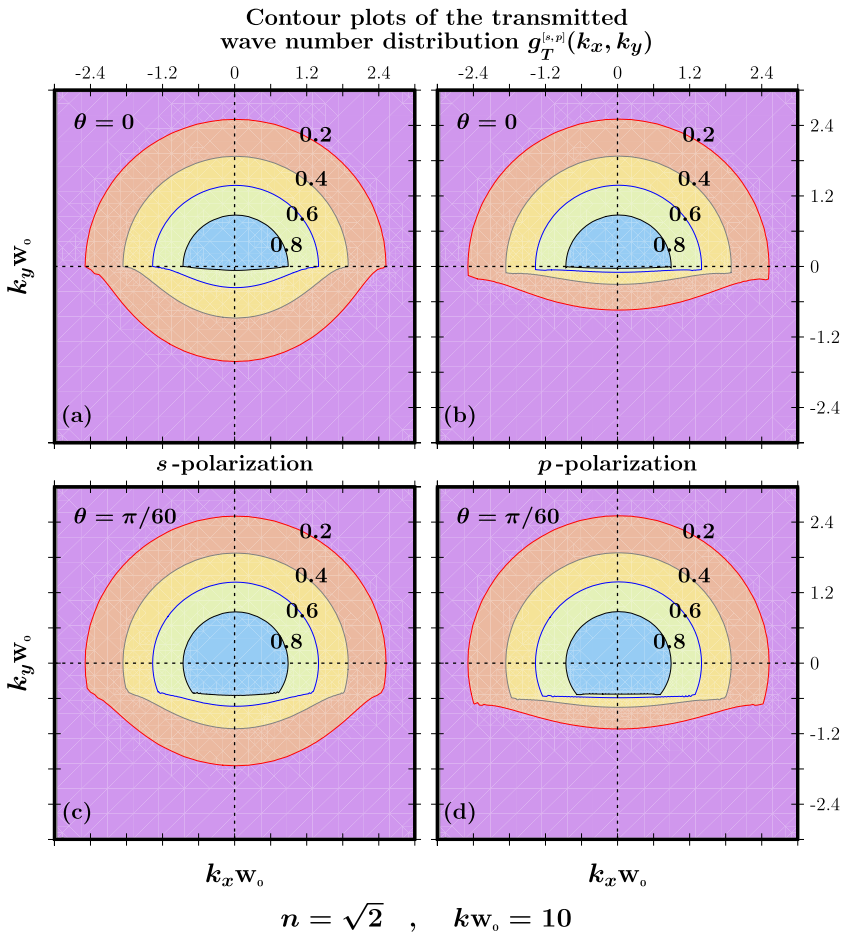

Figure 3. Contour plots of the transmitted wavenumber distribution, $g_T(k_x, k_y)$, for $kw_0 = 10$ and for increasing values of the incidence angle. The numerical data show that the symmetry, which is broken for $\theta = 0$, is recovered by increasing the value of θ (total internal reflection).

the critical angle (see figure 3), the symmetry between k_x and k_y in the wavenumber distribution is broken. As anticipated in section 1, this *symmetry breaking* is responsible for the creation of a *dynamical* maximum. To examine this phenomenon in detail, let us first consider incidence at $\theta = \pi/4$:

$$\mathcal{F}^{[s,p]}_{\frac{\pi}{4}}(y,z) = \frac{w_0}{2\sqrt{\pi}} \int_{-\infty}^{+\infty} dk_y \, T^{[s,p]}_{\frac{\pi}{4}}(0,k_y) \times \exp\left[-\frac{k_y^2 w_0^2}{4} - ik_y y - i\frac{k_y^2}{2k} z\right]. \quad (24)$$

To estimate the maximum, we can apply the stationary phase method [5]:

$$0 = \left\{ \frac{\partial}{\partial k_y} \left[\text{phase}\left[T^{[s,p]}_{\frac{\pi}{4}}(0,k_y) \right] - k_y y - \frac{k_y^2}{2k} z \right] \right\}_{ky=\langle ky \rangle}.$$

Due to the fact that the phase of the transmission coefficient $T^{[s,p]}_{\theta}(0,k_y)$ is not dependent on the spatial coordinates, we can immediately find an analytical expression for the shift in y between two maxima, i.e.

$$\Delta y = -\frac{\langle k_y \rangle}{k} \Delta z. \quad (25)$$

For $\theta = \pi/4$, $n = \sqrt{2}$, and $kw_0 \geq 10$, the wavenumber distribution is a symmetric distribution centered at $k_y = 0$. Consequently, $\langle k_y \rangle = 0$ and the maximum does *not* change its position. We thus recognize a *stationary* maximum. The numerical analysis confirms this theoretical prediction; see figure 4.

Let us now consider incidence at the critical angle:

$$\sin\theta_c + \sqrt{n^2 - \sin^2\theta_c} = \sqrt{2}.$$

For $n = \sqrt{2}$ the critical angle is $\theta_c = 0$ and the transverse y–z profile is determined by

$$\mathcal{F}^{[s,p]}_{0}(y,z) = \frac{w_0}{2\sqrt{\pi}} \int_{-\infty}^{+\infty} dk_y \, T^{[s,p]}_{0}(0,k_y) \times \exp\left[-\frac{k_y^2 w_0^2}{4} + ik_y z - i\frac{k_y^2}{2k} y\right]. \quad (26)$$

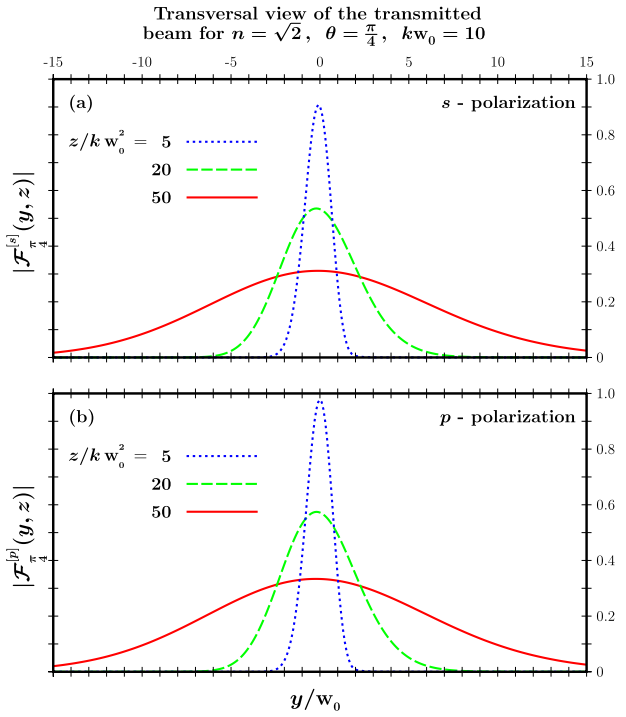

Figure 4. Transverse view of the transmitted beam for s- and p-polarized waves, $\mathcal{F}^{[\mathrm{s,p}]}_{\frac{\pi}{4}}(y,z)$. Due to the symmetry of the transmitted wavenumber distribution, we find *stationary* maxima.

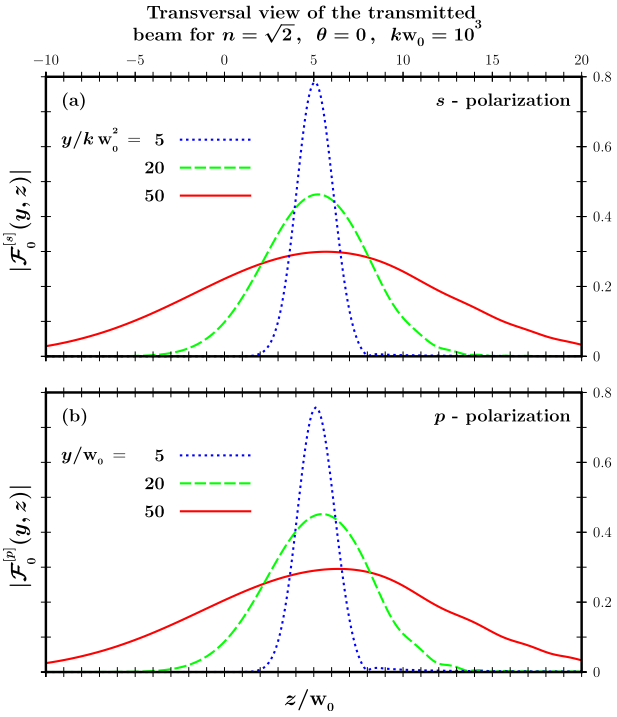

Figure 5. Transverse view of the transmitted beam for s- and p-polarized waves at the critical angle, $\mathcal{F}^{[s,p]}_{0}(y,z)$, for $k\mathrm{w}_0=10^3$. Due to the *partial* breaking of symmetry of the transmitted wavenumber distribution, we see the first modifications of the transmitted beam.

In this case, the z-shift of the maximum in terms of the y-location of the detector is given by

$$\Delta z=\frac{\langle k_y\rangle}{k}\Delta y. \tag{27}$$

For $k\mathrm{w}_0=10^3$, the wavenumber distribution is not completely symmetric in k_y and this produces the first modifications of the transmitted beam; see figure 5. So small a modification is more evident for p-polarized waves. On decreasing the value of $k\mathrm{w}_0$ up to 10, we lose the symmetry (see figure 2) and we clearly find a *dynamical* maximum. To estimate this dynamical shift, we observe that, as seen in section 1, for $k\mathrm{w}_0=10$ only positive values of k_y contribute to the mean value; this implies

$$\langle k_y\rangle=\frac{2}{\mathrm{w}_0\sqrt{\pi}} \tag{28}$$

and, consequently, the shift in z of the transmitted optical beam is given by

$$\Delta z=\frac{2}{k\mathrm{w}_0\sqrt{\pi}}\Delta y. \tag{29}$$

The numerical analysis, shown in figure 6, confirms this prediction. In such a plot, the *asymmetric* interference which appears in the presence of dynamical maxima is also clear.

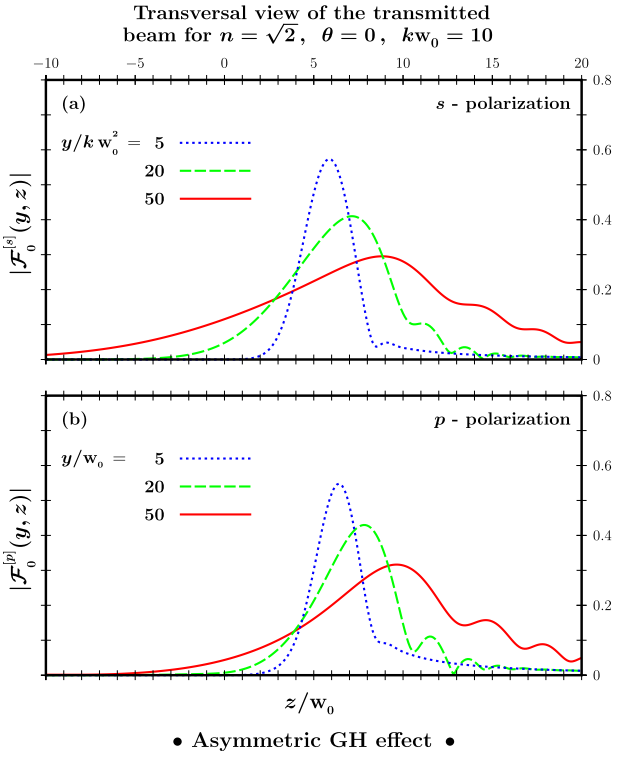

Figure 6. Transverse view of the transmitted beam for s- and p-polarized waves at the critical angle, $\mathcal{F}^{[s,p]}_{0}(y,z)$, for $k\mathrm{w}_0=10$. Due to the *total* breaking of symmetry of the transmitted wavenumber distribution, the phenomena of dynamical shift and asymmetric interference appear clearly.

4. Conclusions

The field of optics is certainly very stimulating as regards reproducing quantum mechanical phenomena. For example,

the well known Goos–Hänchen shift [11] is the optical analogy of the *delay* time in non-relativistic quantum mechanics [3, 13]. These optical and quantum effects arise due to the fact that evanescent waves exist in the classical forbidden region. This intriguing shift, which is a constant matter of scientific investigation [16–19], is, in general, a *stationary* shift. In this paper, we have analyzed in which situations this stationary shift becomes a *dynamical* shift.

Due to the fact that the dynamical shift is a direct consequence of the breaking of symmetry in the wavenumber distribution, this new optical phenomenon can also be seen as an *asymmetric* GH effect. In our study, we have seen that more convenient circumstances for reproducing this *new* phenomenon are the choices of incidence at critical angles and of beam waists of $w_0 \approx 10/k \approx 1.6\lambda$, of the order of the wavelength of the incoming Gaussian beam. This seems to be too restrictive for a possible experimental implementation of the theoretical analysis presented in this paper. Nevertheless, this difficulty is very similar to the difficulty found in detecting the standard Goos–Hänchen shift, which is of the order of the wavelength of the incoming beam. Consequently, it can be overcome with the same trick, i.e. *amplifying* the shift. For example, by preparing a dielectric structure which allows $2N + 1$ internal reflections, we obtain for the transmission coefficient the following expressions:

$$\left|T_\theta^{[s,2N+1]}(k_x, k_y)\right| = \frac{4k_{z_{\text{in}}} q_{z_{\text{in}}}}{(k_{z_{\text{in}}} + q_{z_{\text{in}}})^2} \left|\frac{q_{z_*} - k_{z_*}}{q_{z_*} + k_{z_*}}\right|^{2N+1} \tag{30}$$

and

$$\left|T_\theta^{[p,2N+1]}(k_x, k_y)\right| = \frac{4n^2 k_{z_{\text{in}}} q_{z_{\text{in}}}}{(n^2 k_{z_{\text{in}}} + q_{z_{\text{in}}})^2} \left|\frac{q_{z_*} - n^2 k_{z_*}}{q_{z_*} + n^2 k_{z_*}}\right|^{2N+1}. \tag{31}$$

At critical angles, we have

$$k_{z_*}^2 > 0 \qquad \text{for } k_y < 0$$

$$\text{and} \qquad k_{z_*}^2 < 0 \qquad \text{for } k_y > 0.$$

Consequently, by increasing the number of internal reflections, we can select the positive k_y-components in the transmitted wavenumber distribution for values of the beam waist, w_0, greater than the wavelength, λ, of the incoming laser beam. The symmetry breaking in the wavenumber distribution, responsible for recovering the second-order k_y-contribution to the phase which contributes to the maximum the term $\langle k_y \rangle y/k$, can thus be optimized for experimental proposals by using the number of internal reflection N and the ratio w_0/λ.

In a forthcoming paper, we shall analyze the asymmetric GH effect for frustrated total internal reflection [23, 24] and resonant photonic tunneling [25]. Another interesting future investigation is represented by the possibility of including the focal shift in our calculation [20]. This additional shift represents a second-order correction to the GH shift and consequently acts as a *delay* in the spreading of the outgoing optical beam.

Acknowledgments

We gratefully thank the Capes (MPA), Fapesp (SAC), and CNPq (SDL) for financial support and the referee for a useful suggestion on amended the title, and for drawing our attention to references on the GH shift and, in particular, on the interesting second-order correction which leads to the focal shift [20].

References

[1] Born M and Wolf E 1999 *Principles of Optics* (Cambridge: Cambridge University Press)
[2] Saleh B E A and Teich M C 2007 *Fundamentals of Photonics* (New York: Wiley)
[3] Tannoudji C C, Diu B and Lalöe F 1977 *Quantum Mechanics* (Paris: Wiley)
[4] Griffiths D J 1995 *Introduction to Quantum Mechanics* (New York: Prentice-Hall)
[5] Dingle R B 1973 *Asymptotic Expansions: their Derivation and Interpretation* (New York: Academic)
[6] Arfken G B and Weber H J 2005 *Mathematical Methods for Physicists* (San Diego, CA: Academic)
[7] Longhi S 2009 Quantum-optical analogies using photonic structures *Laser Photon. Rev.* **3** 243–61
[8] De Leo S and Rotelli P 2008 Localized beams and dielectric barriers *J. Opt.* A **10** 115001
[9] De Leo S and Rotelli P 2011 Laser interaction with a dielectric block *Eur. Phys. J.* D **61** 481–8
[10] Carvalho S and De Leo S 2013 Resonance, multiple diffusion and critical tunneling for Gaussian lasers *Eur. Phys. J.* D **67** 168–11
[11] Goos F and Hänchen H 1947 Ein neuer und fundamentaler Versuch zur Totalreflexion *Ann. Phys.* **436** 333–46
[12] Horowitz B R and Tamir T 1971 Lateral displacement of a light beam at a dielectric interface *J. Opt. Soc. Am.* **61** 586–94
[13] Yasumoto K and Oishi Y 1983 A new evaluation of the Goos–Hänchen shift and associated time delay *J. Appl. Phys.* **54** 2170–6
[14] Seshadri S R 1988 Goos–Hänchen beam shift at total internal reflection *J. Opt. Soc. Am.* A **5** 583–5
[15] Broe J and Keller O 2002 Quantum-well enhancement of the Goos–Hänchen shift for *p*-polarized beams in a two-prism configuration *J. Opt. Soc. Am.* A **19** 1212–22
[16] Aiello A 2012 Goos–Hänchen and Imbert–Fedorov shifts: a novel perspective *New J. Phys.* **14** 013058
[17] Prajapati C and Ranganathan D 2012 Goos–Hänchen and Imbert–Fedorov shifts for Hermite–Gauss beams *J. Opt. Soc. Am.* A **29** 1377–82
[18] Dennis M R and Götte J B 2012 The analogy between optical beam shifts and quantum weak measurements *New J. Phys.* **14** 073013
[19] Bliokh K Y and Aiello A 2013 Goos–Hänchen and Imbert–Fedorov beam shifts: an overview *J. Opt.* **15** 014001
[20] McGuirk M and Carniglia C K 1977 An angular spectrum representation approach to the Goos–Hänchen shift *J. Opt. Soc. Am.* **67** 103–7
[21] Lai H M, Cheng F C and Tang W K 1986 Goos–Hänchen effect around and off the critical angle *J. Opt. Soc. Am.* A **3** 550–7
[22] Chan C C and Tamir T 1987 Beam phenomena at and near critical incidence upon a dielectric interface *J. Opt. Soc. Am.* A **4** 656–63
[23] Haibel A, Nimtz G and Stahlhofen A A 2001 Frustrated total internal reflection: the double prism revisited *Phys. Rev.* E **63** 047601
[24] Carvalho S and De Leo S 2013 Light transmission through a triangular air gap *J. Mod. Opt.* **60** 437–43
[25] De Leo S and Rotelli P 2011 Resonant laser tunneling *Eur. Phys. J.* D **65** 563–70